Check for updates

American Society of Hematology
2021 L Street NW, Suite 900,
Washington, DC 20036
Phone: 202-776-0544 | Fax 202-776-0545
editorial@hematology.org

Mammalian VPS45 orchestrates trafficking through the endosomal system

Tracking no: BLD-2020-006871R2

Laura Frey (Dr. von Hauner Children's Hospital, Germany) Natalia Zietara (Ludwig-Maximilians-Universität München, Germany) Marcin Lyszkiewicz (LMU Munchen, Germany) Benjamin Marquardt (Ludwig-Maximilians-Universität München, Germany) Yoko Mizoguchi (Ludwig-Maximilians-Universität München, Germany) Monika Linder (Ludwig-Maximilians-Universität München, Germany) Yanshan Liu (Ludwig-Maximilians-Universität München, Germany) Florian Giesert (Helmholtz Zentrum München, Germany) Wolfgang Wurst (Helmholtz Zentrum München, Germany) Maik Dahlhoff (Ludwig-Maximilians-Universität München, Germany) Marlon Schneider (Ludwig-Maximilians-Universität München, Germany) Eckhard Wolf (Ludwig-Maximilians-Universität München, Germany) Raz Somech (Edmond and Lily Safra Children's Hospital, Sheba Medical Center, affiliated to Tel Aviv University, Israel) Christoph Klein (Dr. von Hauner Childrens Hospital, LMU Klinikum, Germany)

Abstract:
Vacuolar protein sorting 45 homolog (VPS45), a member of the Sec1/Munc18 (SM) family, has been implicated in the regulation of endosomal trafficking. VPS45 deficiency in human patients results in congenital neutropenia, bone marrow fibrosis, and extramedullary renal hematopoiesis. Detailed mechanisms of the VPS45 function are unknown. Here, we show an essential role of mammalian VPS45 in maintaining the intracellular organization of endolysosomal vesicles and promoting recycling of cell-surface receptors. Loss of VPS45 causes defective Rab5-to-Rab7 conversion resulting in trapping of cargos in early endosomes and impaired delivery to lysosomes. In this context, we demonstrate aberrant trafficking of the G-CSF receptor (G-CSFR) in the absence of VPS45. Furthermore, we find that lack of VPS45 in mice is not compatible with embryonic development. Thus, we identify mammalian VPS45 as a critical regulator of trafficking through the endosomal system and early embryogenesis of mice.

Conflict of interest: No COI declared

COI notes:

Preprint server: No;

Author contributions and disclosures: L.F., N.Z., M.Ł., and C.K. designed the research; L.F. conducted experiments and analyzed the data; Y.M. generated genetically modified iPSCs; M.I.L. assisted in iPSCs differentiation; B.M. and Y.L. assisted in molecular cloning and CRISPR/Cas9-mediated gene editing; F.G. and W.W. performed mouse rederivation by IVF and helped with the embryo analysis, M.D., M.R.S., and E.W. generated the KO mice; R.S. provided critical interpretation of the data; N.Z., M.Ł., and C.K. conceived the study design and supervised L.F.; L.F. wrote the manuscript; N.Z., M.Ł., and C.K. revised the manuscript. All authors approved the final version of the manuscript.

Non-author contributions and disclosures: No;

Agreement to Share Publication-Related Data and Data Sharing Statement: For original data, please contact Christoph.Klein@med.uni-muenchen.de

Clinical trial registration information (if any):

Downloaded from http://ashpublications.org/blood/article-pdf/doi/10.1182/blood.2020006871/1795769/blood.2020006871.pdf by HELMHOLTZ ZENTRUM user on 16 February 2021

Mammalian VPS45 orchestrates trafficking through the endosomal system

Laura Frey[1], Natalia Ziętara[1], Marcin Łyszkiewicz[1], Benjamin Marquardt[1], Yoko Mizoguchi[1], Monika I. Linder[1], Yanshan Liu[1], Florian Giesert[2], Wolfgang Wurst[2], Maik Dahlhoff[3], Marlon R. Schneider[3], Eckhard Wolf[3], R. Somech[4], Christoph Klein[1]

1) Department of Pediatrics, Dr. von Hauner Children's Hospital, Ludwig-Maximilians-Universität München, Munich, Germany; 2) Institute of Developmental Genetics, Helmholtz Zentrum München, German Research Center for Environmental Health GmbH, Neuherberg, Germany; 3) Institute of Molecular Animal Breeding and Biotechnology, Gene Center, Ludwig-Maximilians-Universität München, Munich, Germany; 4) Pediatric Department A and the Immunology Service, Jeffrey Modell Foundation Center, "Edmond and Lily Safra" Children's Hospital, Sheba Medical Center, Tel Hashomer, Sackler Faculty of Medicine, Tel Aviv University, Israel.

Correspondence: Christoph Klein, Department of Pediatrics, Dr. von Hauner Children's Hospital, Ludwig-Maximilians-Universität München, Lindwurmstraße 4, 803377 Munich, Germany, e-mail: Christoph.Klein@med.uni-muenchen.de, phone: +49 (0)89-4400-57701, fax: +49 (0)89-4400-57702.

Downloaded from http://ashpublications.org/blood/article-pdf/doi/10.1182/blood.2020006871/1795769/blood.2020006871.pdf by HELMHOLTZ ZENTRUM user on 16 February 2021

Key points:

- VPS45 is required for endocytic trafficking of G-CSFR and other cargos
- VPS45 is fundamental for early embryogenesis of mouse

Abstract

Vacuolar protein sorting 45 homolog (VPS45), a member of the Sec1/Munc18 (SM) family, has been implicated in the regulation of endosomal trafficking. VPS45 deficiency in human patients results in congenital neutropenia, bone marrow fibrosis, and extramedullary renal hematopoiesis. Detailed mechanisms of the VPS45 function are unknown. Here, we show an essential role of mammalian VPS45 in maintaining the intracellular organization of endolysosomal vesicles and promoting recycling of cell-surface receptors. Loss of VPS45 causes defective Rab5-to-Rab7 conversion resulting in trapping of cargos in early endosomes and impaired delivery to lysosomes. In this context, we demonstrate aberrant trafficking of the G-CSF receptor (G-CSFR) in the absence of VPS45. Furthermore, we find that lack of VPS45 in mice is not compatible with embryonic development. Thus, we identify mammalian VPS45 as a critical regulator of trafficking through the endosomal system and early embryogenesis of mice.

Downloaded from http://ashpublications.org/blood/article-pdf/doi/10.1182/blood.2020006871/1795769/blood.2020006871.pdf by HELMHOLTZ ZENTRUM user on 16 February 2021

Introduction

Patients with loss-of-function variants in *VPS45* present with infections due to severe neutropenia, progressive bone marrow fibrosis, and nephromegaly secondary to extramedullary hematopoiesis [1,2]. VPS45 deficiency is further characterized by an impaired migration and increased apoptosis of neutrophil granulocytes. Notably, patients are refractory to the treatment with granulocyte colony-stimulating factor (G-CSF), even in high doses [1,2].

VPS45 is involved in the endocytic pathway, which controls numerous cellular functions [3–5] and is composed of various specialized compartments that are interconnected by vesicle flux [6,7]. The first step of the endocytic pathway is the uptake of cargo material into pre-existing early endosomes [8,9]. Early endosomes function as sorting platforms, from which cargo is either recycled or destined for degradation [10,11].

The endosomal system is highly dynamic and cargo transport along the endocytic route requires tight coordination. Rab GTPases and their effectors are critical regulators of the transport machinery [12–14]. The small GTPase Rab5 governs vesicle fusion and intracellular organization of early endosomes [15–17], whereas the GTPase Rab7 controls late endocytic traffic [18]. By gradually replacing Rab5 by Rab7, early endosomes mature into late endosomes [19,20]. Upon fusion of late endosomes with lysosomes, cargo is proteolytically degraded in the lysosomal compartment. Conversely, recycling of cargo from Rab5-positive early endosomes to the cell surface is regulated by the GTPases Rab4 and Rab11, which characterize the fast and the slow recycling pathways, respectively [21–23]. Due to its function as a dual Rab5 and Rab4 effector, Rabenosyn-5 plays a key role in the endocytic pathway [24,25]. Besides Rab GTPases, Sec1/Munc18 (SM) proteins are essential to execute membrane fusion events by binding soluble N-ethylmaleimide-sensitive-factor attachment receptors (SNAREs) [26]. The evolutionarily conserved VPS45 protein is a member of the SM family and plays a crucial role in vesicle-mediated transport through the endosomal network. Mammalian VPS45 directly binds to Rabenosyn-5 [25] as well as the SNARE protein Syntaxin16 [27] and the interaction is conserved in species including *Saccharomyces*

Downloaded from http://ashpublications.org/blood/article-pdf/doi/10.1182/blood.2020006871/1795769/blood.2020006871.pdf by HELMHOLTZ ZENTRUM user on 16 February 2021

cerevisiae, *Drosophila sp.,* and *Caenorhabditis elegans* [28–31]. Studies in yeast suggest a role of Vps45p in the transport of vesicles from the Golgi apparatus to the prevacuolar compartment [32–34]. Moreover, a function in cargo internalization and endosome formation has been ascribed to Vps45 in *Drosophila* and *C. elegans* [29,30] and human VPS45 has been implicated in the recycling of beta 1 integrin [35].

The precise function of the SM protein VPS45 in endosomal trafficking and its significance for mammalian development are not yet understood. In this study, we investigate the role of VPS45 in the endocytic pathway *in vitro* and *in vivo.*

Downloaded from http://ashpublications.org/blood/article-pdf/doi/10.1182/blood.2020006871/1795769/blood.2020006871.pdf by HELMHOLTZ ZENTRUM user on 16 February 2021

Methods

Further details regarding the methods used are provided in the supplemental methods.

Live cell imaging of endosome maturation

HeLa cells expressing mCherry-Rab5 and mCerulean-Rab7 were cultured in glass bottom dishes (ibidi, 35 mm # 1.5H) and incubated with fluorescent microspheres (FluoSpheres, carboxylate-modified microspheres, 0.02 µm, dark red fluorescent, Thermo Fisher Scientific) for 10 minutes at 37 °C to allow uptake. Plates were washed twice and imaged in DMEM on a microscope stage at 37 °C, 5% CO_2 in a humidified atmosphere using Zeiss LSM 800 confocal microscope using the Axio Observer.Z1/7 and a Plan-Apochromat 63x/1.4 oil immersion objective. Images were acquired every 12 seconds up to 90 minutes using bidirectional scanning and 1x line averaging.

Uptake and processing of cargo proteins

HeLa cells were incubated with either 32.5 µg/ml Alexa Fluor 488-conjugated ovalbumin (OVA-488, Thermo Fisher Scientific), 65 µg/ml of DQ ovalbumin (DQ OVA, Thermo Fisher Scientific), 65 µg/ml DQ Green BSA (Thermo Fisher Scientific) or 65 µg/ml pHrodo Green dextran (Thermo Fisher Scientific) for various periods at 37 °C. Cargo uptake and processing was stopped by washing the cells twice with ice-cold PBS. The rate of cargo uptake and processing was determined by flow cytometry as a change in MFI from baseline (fluorescence at 4 °C). When indicated, cells were treated with 25 µM chloroquine (CQ, Sigma-Aldrich). Alternatively, cells were processed for confocal microscopy.

EGFR trafficking assay

HeLa cells were serum-starved prior to stimulation with 100 ng/ml human EGF (Thermo Fisher Scientific) for various time periods. Cells were washed twice in PBS and processed for immunoblotting or confocal microscopy.

G-CSFR trafficking assay

Downloaded from http://ashpublications.org/blood/article-pdf/doi/10.1182/blood.2020006871/1795769/blood.2020006871.pdf by HELMHOLTZ ZENTRUM user on 16 February 2021

HeLa cells were transduced with G-CSFR-GFP fusion constructs and sorted to achieve equal expression levels. Cells were serum-starved, stimulated with 100 ng/ml recombinant human G-CSF (PeproTech) for various time periods, washed twice in PBS, fixed and processed for confocal microscopy.

Downloaded from http://ashpublications.org/blood/article-pdf/doi/10.1182/blood.2020006871/1795769/blood.2020006871.pdf by HELMHOLTZ ZENTRUM user on 16 February 2021

Results

VPS45 controls the intracellular organization of endolysosomal vesicles

To examine the function of human VPS45 in the endocytic system, we first generated clonal *VPS45* knockout (KO) HeLa and PLB-985 cells using CRISPR/Cas9-mediated gene editing by targeting exon 7 of *VPS45* (Supplemental Figure 1A). Loss of *VPS45* expression resulted in a markedly reduced abundance of its interacting proteins Rabenosyn-5 and Syntaxin16 in both cell lines (Figure 1A and Supplemental Figure 1B), demonstrating that VPS45 impacts on the expression of its interaction partners.

Next, we studied the morphology and distribution of various types of intracellular vesicles. In striking contrast to control cells, in which the early endosomal marker EEA1 revealed a typical punctate distribution throughout the cytoplasm, EEA1-positive early endosomes were aggregated in *VPS45* KO cells. Similarly, late endosomes expressing LAMP2 showed an aberrant morphology with clustered and enlarged vesicles. In addition, VPS45 deficiency resulted in an accumulation of LAMP1-positive lysosomes (Figure 1B). Despite the clustering of endosomal and lysosomal vesicles, the overall expression levels of EEA1, LAMP2, and LAMP1 were not altered in *VPS45* KO cells (Figure 1C). These results document an essential role of VPS45 in maintaining the intracellular organization of endolysosomal vesicles.

Cargo recycling but not internalization and mitochondrial function depend on VPS45

To examine whether VPS45 deficiency also impairs cargo transport through these compartments, we tested the internalization, recycling, and degradation of various proteins. Both control and *VPS45* KO cells were capable to endocytose fluorescent cargo at comparable rates over time, indicating that VPS45 is dispensable for cargo internalization (Figure 2A). In addition, the absence of VPS45 did not impact on mitochondrial function (Supplemental Figures 2A-B).

Downloaded from http://ashpublications.org/blood/article-pdf/doi/10.1182/blood.2020006871/1795769/blood.2020006871.pdf by HELMHOLTZ ZENTRUM user on 16 February 2021

Since the inactivation of VPS45 results in the reduced expression of the dual Rab4 and Rab5 effector Rabenosyn-5, we hypothesized that both Rab4- and Rab5-controlled recycling and degradative pathways might be affected in the absence of VPS45. The transferrin receptor and its ligand transferrin are widely used to study the recycling pathway. Control cells efficiently recycled transferrin while VPS45 deficiency caused a delay in fast transferrin recycling (Figure 2B). An intracellular accumulation of transferrin after 10 and 30 minutes of recycling was also observed in *VPS45* KO cells compared to control cells by confocal microscopy (Supplemental Figure 2C). Endogenous expression levels of Rab4 and Rab11 were not affected by the depletion of VPS45 (Supplemental Figure 2D). Thus, inactivation of *VPS45* delays recycling of transferrin through the early endosomal sorting station.

VPS45 depletion disrupts cargo degradation and delays maturation of cathepsin D

To further evaluate whether the degradation pathway is affected in the absence of VPS45, we tested the transport of cargo destined for lysosomal processing using three distinct compounds. DQ Ovalbumin (DQ OVA) and DQ Green BSA exhibit fluorescence upon proteolytic processing in low pH compartments, whereas pHrodo Green dextran is pH-sensitive and generates increasing amounts of fluorescent peptides with decreasing pH. Confocal microscopy analysis revealed efficient processing of DQ OVA in LAMP2-positive late endosomes in control cells after 90 minutes of incubation, whereas markedly less DQ OVA punctae were observed in *VPS45* KO cells (Figure 3A). These results are in line with the reduced degradative capacity of *VPS45* KO cells measured by flow cytometry (Figures 3B-D). Since *VPS45* KO cells were capable of efficient compound uptake (Figure 2A), it is likely that post-endocytic steps in the degradative pathway are affected. To further test the hypothesis of impaired fusion of endolysosomal vesicles, cells were additionally treated with chloroquine (CQ), a lysosomotropic component which raises the lysosomal pH and affects fusion activity [36–38]. CQ treatment reduced DQ OVA fluorescence in control cells to the level of *VPS45* KO cells, whereas it did not affect cargo degradation by *VPS45* KO cells (Figure

Downloaded from http://ashpublications.org/blood/article-pdf/doi/10.1182/blood.2020006871/1795769/blood.2020006871.pdf by HELMHOLTZ ZENTRUM user on 16 February 2021

3B). These results indicate a decreased degradative capacity in the absence of VPS45, consistent with a defective fusion of endolysosomal vesicles.

Expression of the mature form of the protease cathepsin D can be used as an indicator of the lysosomal pH and proteolytic capacity, as the conversion of cathepsin D from the 53 kD immature and 47 kD intermediate forms to the 31 kD mature form requires transport to late endosomes or lysosomes and an appropriate acidic milieu. Whereas mature forms of cathepsin D were virtually absent, immature forms accumulated in *VPS45* KO cells (Figure 3E). These results are in line with the reduced protein degradation capacity and could reflect an inefficient delivery of proteases from the Golgi apparatus to endolysosomal vesicles in the absence of VPS45. Of note, the maturation of cathepsin D was further inhibited by incubation with CQ, indicating that lysosomal transport and biogenesis are not merely dependent on VPS45 (Supplemental Figure 3).

Epidermal growth factor receptor (EGFR) is accumulated in early endosomes in the absence of VPS45

Next, we examined trafficking of EGFR, a model receptor that is used to study trafficking along the degradative pathway. In control cells, a substantial degradation of receptors was observed over time. In contrast, deletion of VPS45 prevented efficient degradation of EGFR (Figure 4A). To gain further insight into EGFR trafficking defects, we visualized the fate of EGFR. After 10 minutes of stimulation, the receptor was enriched in EEA1-positive early endosomes in both control and *VPS45* KO cells, indicating an intact internalization. After 90 minutes, EGFR signals revealed reduced co-localization with EEA1-positive endosomes and an overall decrease in control cells, suggesting an efficient exit of the cargo from early endosomes. In contrast, EGFR remained captured in EEA1-positive vesicles in *VPS45* KO cells over time (Figures 4B-C). These data suggest that VPS45 facilitates the fusion of early endosomal and lysosomal vesicles.

Lack of VPS45 causes trapping of granulocyte colony-stimulating factor receptor (G-CSFR) in early endosomes and hampered delivery to late endosomes

Downloaded from http://ashpublications.org/blood/article-pdf/doi/10.1182/blood.2020006871/1795769/blood.2020006871.pdf by HELMHOLTZ ZENTRUM user on 16 February 2021

Patients with loss-of-function variants in *VPS45* are neutropenic and refractory to G-CSF treatment [1,2]. Our data demonstrate an impaired endolysosomal vesicle fusion in the absence of VPS45. Hence, we hypothesized that hyporesponsiveness to G-CSF is caused by impaired trafficking of G-CSFR. Upon ligand-binding, G-CSFR is internalized and transported to early endosomes, where the majority of the receptor-ligand complex is sorted for lysosomal degradation [39]. After 30 minutes of stimulation, the G-CSFR/G-CSF complex reached EEA1-positive early endosomes in both control and *VPS45* KO cells. Whereas G-CSFR co-localized with LAMP2-positive late endosomes after 30 and 90 minutes in control cells, trafficking to late endosomes was impaired in *VPS45* KO cells, which showed a sustained accumulation of receptors in early endosomes instead (Figures 5A-B). Of note, receptor mistrafficking did not impact markedly on signaling, as G-CSFR- and GM-CSFR-mediated signaling seemed to be intact in the absence of VPS45 (Supplemental Figures 4A-C). However, more studies are required to study the potential impact of G-CSFR mistrafficking on the refractoriness of VPS45-deficient patients to G-CSF therapy in depth.

VPS45 depletion results in defective endosome maturation

Endosome maturation ensures that cellular cargo targeted for degradation reaches the lysosomal compartment. This process is defined by the conversion of early endosomal Rab5 to late endosomal Rab7 [19]. We observed the arrest of internalized cargo proteins and receptors in early endosomes in the absence of VPS45, suggesting an impaired endosome maturation. Of note, endogenous levels of Rab5 and Rab7 were not affected in *VPS45* KO cells (Supplemental Figure 5). To further assess whether the switch of Rab5 to Rab7 is affected in *VPS45* KO cells, the fate of fluorescent cargo was monitored by live cell imaging in control and *VPS45* KO cells co-expressing mCherry-Rab5 and mCerulean-Rab7. Notably, the overall appearance of early and late endosomal vesicles differed between control and *VPS45* KO cells. Ring-shaped structures for both Rab5- and Rab7-positive vesicles were only observed in control cells (Figure 6A). In *VPS45* KO cells, vesicles were aggregated and disorganized, like vesicles marked by EEA1, LAMP2 and LAMP1 proteins (Figure 1B).

Downloaded from http://ashpublications.org/blood/article-pdf/doi/10.1182/blood.2020006871/1795769/blood.2020006871.pdf by HELMHOLTZ ZENTRUM user on 16 February 2021

In control cells, a continuous decline in the early endosomal marker Rab5 and a gradual increase in the late endosomal marker Rab7 on cargo vesicles was observed over time. Eventually, Rab5 completely dissociated from the cargo while being replaced by Rab7, indicative of complete endosome maturation (Figures 6A-B and Supplemental Video 1). In *VPS45* KO cells, cargo was transported to Rab5-positive vesicles. Even though we observed that Rab7 appeared on Rab5-positive endosomes, Rab7 recruitment was slower in comparison to control cells. Importantly, in contrast to control cells, Rab5 did not disappear from the cargo vesicle in *VPS45* KO cells, suggesting that endosome maturation was never fully completed (Figures 6A-B and Supplemental Video 2). These data show that VPS45 is required for early-to-late endosome conversion and efficient cargo delivery to the degradative compartment.

Alleles carrying patient-associated *VPS45* variants are hypomorphic

In contrast to the full *VPS45* KO in engineered HeLa cells, patients with biallelic point variants in the *VPS45* gene retain some residual protein expression. It is unclear to which degree variant VPS45 proteins are still functional. To further investigate the effects of the patient-associated Glu238Lys and Thr224Asn variants on the VPS45 proteins we analyzed their subcellular localization. Confocal microscopy analysis revealed no difference in localization between control and variant VPS45 proteins (Supplemental Figure 6A).

We next investigated whether these variants abolish the interaction of VPS45 with the known binding partners Rabenosyn-5 and Syntaxin16. HEK293T cells were transiently transfected with C-terminally FLAG-tagged control or variant VPS45 plasmids. In these cells, we found that variant VPS45 was significantly less abundant than control VPS45 (Supplemental Figure 6B). Co-purification results confirmed interactions of control VPS45 with Rabenosyn-5 and Syntaxin16, respectively. Moreover, variant VPS45 proteins were able to pull down both interaction partners, albeit to a lesser degree (Supplemental Figure 6C). These results indicate that the interactions of variant VPS45 and binding partners are not completely abolished. Importantly, degradation rates of DQ OVA were restored by overexpressing either

Downloaded from http://ashpublications.org/blood/article-pdf/doi/10.1182/blood.2020006871/1795769/blood.2020006871.pdf by HELMHOLTZ ZENTRUM user on 16 February 2021

control or variant versions of VPS45 in KO cells (Supplemental Figure 6D), suggesting that the alleles in VPS45-deficient patients are hypomorphic.

By introducing the patient-specific Thr224Asn variant into induced pluripotent stem cells (iPSCs), we further analyzed its effect on neutrophil development. During *in vitro* differentiation, the expression of stemness-related and granule genes as well as the percentage of CD33lowCD11b+ were comparable in control and *VPS45* KI neutrophils (Supplemental Figures 7A-C), however, significantly fewer live floating cells were counted in wells containing *VPS45* KI colonies, indicating a reduced capacity to generate neutrophils (Supplemental Figure 7D). This is in line with the observation of multiple apoptotic cells in these cells by confocal microscopy. In non-apoptotic cells, the cytoplasmic localization of neutrophil elastase, a protein frequently mutated in SCN, was similar for both genotypes (Supplemental Figure 7E). Of note, the generation of VPS45 KO iPSCs was not successful, indicating that a complete loss might be lethal.

Lack of VPS45 in mouse development is lethal at around E7.5

To further explore the biological relevance of VPS45 in a mammalian *in vivo* model, we generated a *Vps45* KO mouse. Since all patient-associated variants maintain partial functionality, we hypothesized that a complete loss of *Vps45* expression might result in embryonic lethality in mice. Therefore, we employed the KO-first strategy to generate the VPS45-deficient mouse model, as this strategy provides the flexibility to rapidly convert the null allele into a conditional allele [41] (Supplemental Figure 8A). 148 female and male pups from 24 litters of heterozygous breeding pairs were genotyped (Figure 7A). Of these pups, 37% (55 mice) were homozygous for the control allele and 63% (93 mice) were heterozygous for the *Vps45* null allele. None of the pups was homozygous for the *Vps45* null allele, indicating that the complete deletion of *Vps45* is embryonic lethal for mice (Figure 7B).

To define the developmental stage at which Vps45 plays an essential role, embryos were analyzed at different days *post-coitum*. Most of the embryos isolated at E11 and E13 showed an age-appropriate development. However, some embryos were markedly smaller and did

Downloaded from http://ashpublications.org/blood/article-pdf/doi/10.1182/blood.2020006871/1795769/blood.2020006871.pdf by HELMHOLTZ ZENTRUM user on 16 February 2021

not develop properly (Figures 7C-D). Genotyping showed that these embryos were homozygous for the *Vps45* null allele (Supplemental Figure 8B). No visible differences in embryo size and shape were detected at E7.5 (Figure 7D). Histological analysis of E7.5 embryos revealed organized embryonic endodermal, mesodermal, and ectodermal structures, suggesting that those embryos are either homozygous for the control allele or heterozygous for the *Vps45* null allele. In contrast, cell layers of suspected *Vps45* KO embryos revealed an overall smaller cell mass and appeared as disorganized structures, making discrimination of germ layers impossible (Figure 7E). Overall, the formation of germ layers appeared to be impaired, pointing towards a defect in the process of gastrulation in the absence of VPS45 [40].

Since the global loss of VPS45 in mice resulted in embryonic lethality at around E7.5 and prevented us from studying the role of VPS45 for neutrophil differentiation, we generated two *Vps45*$^{fl/fl;LysM\text{-}Cre}$ or *Vps45*$^{fl/fl;Vav\text{-}Cre}$ conditional KO mouse lines to deplete VPS45 in the myeloid and hematopoietic compartments respectively. However, VPS45 was inefficiently deleted in sorted neutrophils of *Vps45*$^{fl/fl;LysM\text{-}Cre}$ and bone marrow cells of *Vps45*$^{fl/fl;Vav\text{-}Cre}$ conditional KO mice and thus precluded further analysis of neutrophil differentiation (Supplemental Figures 8C-D).

VPS45 depletion delays neutrophil differentiation *ex vivo*

To circumvent the obstacle of studying neutrophil differentiation *in vivo*, we opted to delete VPS45 *ex vivo* using Cre-expressing retroviral vectors. Cre-expressing myeloid CD11b+Gr1+ cells carrying homozygous floxed, heterozygous floxed or homozygous control *Vps45* alleles showed lowest, intermediate and highest *Vps45* mRNA levels, respectively (Supplemental Figure 9A). Generally, the percentage of Cre-positive neutrophils declined over time, consistent with Cre-mediated cellular toxicity. Numbers of VPS45-depleted neutrophils significantly decreased at day 4 of co-culture and a further decline was observed at day 7 as compared to control cells (Supplemental Figures 9B-C). Insufficient *Vps45* expression may

Downloaded from http://ashpublications.org/blood/article-pdf/doi/10.1182/blood.2020006871/1795769/blood.2020006871.pdf by HELMHOLTZ ZENTRUM user on 16 February 2021

have led to increased cell death or a halt in differentiation. These results stress the significance of VPS45 for neutrophil differentiation.

Downloaded from http://ashpublications.org/blood/article-pdf/doi/10.1182/blood.2020006871/1795769/blood.2020006871.pdf by HELMHOLTZ ZENTRUM user on 16 February 2021

Discussion

In this study we report a novel role of VPS45 in regulating endocytic trafficking, particularly the fusion of early endosomes. Complete loss of VPS45 results in the perturbed intracellular organization of endolysosomal vesicles and cargo mistrafficking through the early endosomal compartment. We demonstrate that VPS45 deficiency causes aberrant trafficking of G-CSFR, which might be associated with the severe neutropenic phenotype of VPS45-deficient patients and their poor response to G-CSF therapy. Importantly, we find that lack of VPS45 is not compatible with life in mouse.

Previous work has shown that a reduction of VPS45 expression due to either patient-associated variants or siRNA-mediated knockdown results in decreased amounts of binding partners Rabenosyn-5 and Syntaxin16 [2,35]. We here confirm that VPS45 regulates the expression levels of these proteins, as Rabenosyn-5 and Syntaxin16 levels are reduced to an even higher extent in the complete absence of VPS45. The VPS45 protein may be critical to stabilize these binding partners and prevent degradation of the complex members via the proteasomal pathway [35]. We assume that reduced amounts of the vesicle fusion machinery components VPS45, Rabenosyn-5, and Syntaxin16 may impede efficient vesicle fusion, resulting in the accumulation of endolysosomal vesicles. This accords with studies in yeast and *Drosophila*, in which large aggregates of potential transport vesicles are found in *Vps45* null cells [30,33], pointing towards an evolutionarily conserved function of VPS45 in fusion events of these cargo vesicles in the endosomal system.

Studies in *Drosophila* and *C. elegans* describe a role of both VPS45 and Rabenosyn-5 in cargo internalization [29,30]. In contrast, we find that VPS45 is dispensable for endocytosis in human cells, since neither clathrin-mediated endocytosis of transferrin, EGFR or G-CSFR nor clathrin-independent uptake of ovalbumin and microspheres are affected in the absence of VPS45. Our results further contradict a study suggesting an impact of VPS45 on uptake and hence mitochondrial function in the pathogenic fungus *Cryptococcus neoformans* [41]. Since we find that lack of VPS45 does not affect uptake in human cells, mitochondrial

Downloaded from http://ashpublications.org/blood/article-pdf/doi/10.1182/blood.2020006871/1795769/blood.2020006871.pdf by HELMHOLTZ ZENTRUM user on 16 February 2021

function remains intact. However, we find that both recycling and degradation pathways are perturbed in *VPS45* KO cells.

The phenotype of *VPS45* KO cells may in part be due to reduced Rabenosyn-5 abundance, known to orchestrate both recycling and degradation pathways. For example, Rabenosyn-5 controls transferrin recycling [42], presumably due to its function as an effector of Rab4, which in turn is known to promote the fast recycling pathway [22,24]. Of note, siRNA-mediated knockdown of Rabenosyn-5 in monkey cells resulted in mislocalization and impaired uptake of transferrin, pointing towards divergent roles of VPS45 and Rabenosyn-5 in the endocytic pathway [42]. Rabenosyn-5 also interacts with EHD1, a protein involved in the slow recycling route [43,44]. Thus, it is plausible that the absence of VPS45 and lower levels of Rabenosyn-5 resulting thereof lead to a delay in transferrin recycling. We also observe vesicle fusion defects at early endosomes, where Rabenosyn-5 is known to act as a Rab5 effector molecule [25]. The switch from early endosomal Rab5 to late endosomal Rab7 is impaired, presumably due to the lack of Rabenosyn-5. Defective endosome maturation results in an accumulation of a variety of cargos in the early endosomal compartment and impaired transfer to the degradative compartment. Likewise, absent VPS45 might impact on the transport and delivery of cathepsin D to the low pH compartment, thus affecting the maturation of the lysosomal protease. Additionally, Syntaxin16 is reported to localize to the Golgi apparatus and to function in the retrograde transport to the TGN [45,46]. Reduced expression of Syntaxin16 could thus affect the mannose 6-dependent transport of the lysosomal protease cathepsin D as well.

Of note, VPS45 and Rabenosyn-5 deficiencies exhibit phenotypic similarities. VPS45-deficient patients suffer from severe neutropenia associated with myelofibrosis [1,2,47]. Similarly, Rabenosyn-5-deficient patients present with syndromic myelofibrosis associated with neutropenia and bone marrow failure [48,49]. VPS45-deficient patients do not respond to G-CSF treatment [1,2,47], a phenotype also observed for Rabenosyn-5-deficient patients [48]. We find that EEA1-positive early endosomes are aggregated in the absence of VPS45 in HeLa

Downloaded from http://ashpublications.org/blood/article-pdf/doi/10.1182/blood.2020006871/1795769/blood.2020006871.pdf by HELMHOLTZ ZENTRUM user on 16 February 2021

cells. Similarly, early endosomes were enlarged and clustered in fibroblasts of Rabenosyn-5-deficient patients [48]. Moreover, transferrin recycling is delayed in *VPS45* KO HeLa cells, which is also the case for fibroblasts derived from Rabenosyn-5-deficient patients [48]. The complete loss of either Rabenosyn-5 (Phenotyping center, Wellcome Trust Sanger Institute) or VPS45 causes preweaning or early embryonic lethality in mice, respectively. Based on our characterization of the variant VPS45 proteins, we assume that they behave as hypomorphs. Overexpression of the variant constructs in *VPS45* KO HeLa cells provides cells with sufficient amounts of partially functional variant VPS45 proteins to restore endosome maturation and cargo delivery to the degradative compartment. In contrast, residual VPS45 levels in patient cells may be too low to efficiently exert function in vesicle transport. At this point, we cannot fully explain to what extent the level of protein expression and the loss-of-function variant contribute to residual VPS45 activity.

In our study we could confirm a critical role of mammalian VPS45 for neutrophil granulocyte differentiation. However, it remains elusive why neutrophils are particularly sensitive to disruption of VPS45-mediated vesicle trafficking. Based on our findings, VPS45 regulates recycling and degradation pathways crucial for multiple immune cells. We would thus expect a broader defect rather than neutropenia. On the other hand, variants in a variety of genes have been identified to affect endosome integrity and to cause severe neutropenia. Human defects in *VPS13B* [50], *RAB27A* [51], and *LAMTOR2* [52] highlight the necessity of proper vesicle trafficking pathways for neutrophil granulocytes. We thus propose that aberrant assembly and fusion of granules with phagolysosomes might be the underlying pathomechanism of VPS45 deficiency, leading to inefficient destruction of engulfed pathogens or dysregulated signaling of receptors.

Taken together, we here demonstrate that loss of VPS45 severely disrupts the intracellular organization of endolysosomal vesicles and interferes with efficient cargo recycling and degradation as well as endosome maturation. VPS45 is critical for early embryonic

Downloaded from http://ashpublications.org/blood/article-pdf/doi/10.1182/blood.2020006871/1795769/blood.2020006871.pdf by HELMHOLTZ ZENTRUM user on 16 February 2021

development in the mouse. Thus, we provide mechanistic insights into a rare hematopoietic disorder characterized by bone marrow fibrosis and congenital neutropenia.

Downloaded from http://ashpublications.org/blood/article-pdf/doi/10.1182/blood.2020006871/1795769/blood.2020006871.pdf by HELMHOLTZ ZENTRUM user on 16 February 2021

Acknowledgments

This work has been supported by grants from the following institutions: the DFG (SFB914 and Gottfried Wilhelm Leibniz Program), the Bundesministerium für Bildung und Forschung (BMBF) (German PID-NET), the Care-for-Rare Foundation, the Deutsches Zentrum für Infektionsforschung (DZIF), and the Elite Network of Bavaria (doctoral program “i-Target”).

Downloaded from http://ashpublications.org/blood/article-pdf/doi/10.1182/blood.2020006871/1795769/blood.2020006871.pdf by HELMHOLTZ ZENTRUM user on 16 February 2021

Contribution: L.F., N.Z., M.Ł., and C.K. designed the research; L.F. conducted experiments and analyzed the data; Y.M. generated genetically modified iPSCs; M.I.L. assisted in iPSCs differentiation; B.M. and Y.L. assisted in molecular cloning and CRISPR/Cas9-mediated gene editing; F.G. and W.W. performed mouse rederivation by IVF and helped with the embryo analysis, M.D., M.R.S., and E.W. generated the KO mice; R.S. provided critical interpretation of the data; N.Z., M.Ł., and C.K. conceived the study design and supervised L.F.; L.F. wrote the manuscript; N.Z., M.Ł., and C.K. revised the manuscript. All authors approved the final version of the manuscript.

Conflict-of-interest disclosure: The authors declare no competing financial interests.

Data sharing: For original data, please email the corresponding author.

Correspondence: Christoph Klein, Department of Pediatrics, Dr. von Hauner Children's Hospital, Ludwig-Maximilians-Universität München, Lindwurmstraße 4, 803377 Munich, Germany, e-mail: Christoph.Klein@med.uni-muenchen.de.

Downloaded from http://ashpublications.org/blood/article-pdf/doi/10.1182/blood.2020006871/1795769/blood.2020006871.pdf by HELMHOLTZ ZENTRUM user on 16 February 2021

References

1. Stepensky P, Saada A, Cowan M, Tabib A, Fischer U, Berkun Y, Saleh H, Simanovsky N, Kogot-Levin A, Weintraub M, Ganaiem H, Shaag A, Zenvirt S, Borkhardt A, Elpeleg O, Bryant NJ, Mevorach D. The Thr224Asn mutation in the VPS45 gene is associated with the congenital neutropenia and primary myelofibrosis of infancy. *Blood*. 2013;121(25):5078-5087.
2. Vilboux T, Lev A, Malicdan MCV, Simon AJ, Järvinen P, Racek T, Puchalka J, Sood R, Carrington B, Bishop K, Mullikin J, Huizing M, Garty BZ, Eyal E, Wolach B, Gavrieli R, Toren A, Soudack M, Atawneh OM, Babushkin T, Schiby G, Cullinane A, Avivi C, Polak-Charcon S, Barshack I, Amariglio N, Rechavi G, van der Werff ten Bosch J, Anikster Y, Klein C, Gahl WA, Somech R. A congenital neutrophil defect syndrome associated with mutations in VPS45. *N Engl J Med*. 2013;369(1):54-65.
3. Sorkin A, Zastrow M von. Endocytosis and signalling: intertwining molecular networks. *Nat Rev Mol Cell Biol*. 2009;10(9):609-622.
4. Maritzen T, Schachtner H, Legler DF. On the move: endocytic trafficking in cell migration. *Cell Mol Life Sci*. 2015;72(11):2119-2134.
5. Saftig P, Klumperman J. Lysosome biogenesis and lysosomal membrane proteins: trafficking meets function. *Nat Rev Mol Cell Biol*. 2009;10(9):623-635.
6. Rothman JE, Wieland FT. Protein sorting by transport vesicles. *Science*. 1996;272(5259):227-234.
7. Chen AH, Silver PA. Designing biological compartmentalization. *Trends Cell Biol*. 2012;22(12):662-670.
8. Mellman I. Endocytosis and molecular sorting. *Annu Rev Cell Dev Biol*. 1996;12:575-625.
9. Doherty GJ, McMahon HT. Mechanisms of endocytosis. *Annu Rev Biochem*. 2009;78:857-902.
10. Mayor S, Presley JF, Maxfield FR. Sorting of membrane components from endosomes and subsequent recycling to the cell surface occurs by a bulk flow process. *J Cell Biol*. 1993;121(6):1257-1269.
11. Jovic M, Sharma M, Rahajeng J, Caplan S. The early endosome: a busy sorting station for proteins at the crossroads. *Histol Histopathol*. 2010;25(1):99-112.
12. Grosshans BL, Ortiz D, Novick P. Rabs and their effectors: Achieving specificity in membrane traffic. *PNAS*. 2006;103(32):11821-11827.
13. Zerial M, McBride H. Rab proteins as membrane organizers. *Nat Rev Mol Cell Biol*. 2001;2(2):107-117.
14. Stenmark H. Rab GTPases as coordinators of vesicle traffic. *Nat Rev Mol Cell Biol*. 2009;10(8):513-525.
15. Gorvel JP, Chavrier P, Zerial M, Gruenberg J. rab5 controls early endosome fusion in vitro. *Cell*. 1991;64(5):915-925.
16. Bucci C, Parton RG, Mather IH, Stunnenberg H, Simons K, Hoflack B, Zerial M. The small GTPase rab5 functions as a regulatory factor in the early endocytic pathway. *Cell*. 1992;70(5):715-728.
17. Zeigerer A, Gilleron J, Bogorad RL, Marsico G, Nonaka H, Seifert S, Epstein-Barash H, Kuchimanchi S, Peng CG, Ruda VM, Del Conte-Zerial P, Hengstler JG, Kalaidzidis Y, Koteliansky V, Zerial M. Rab5 is necessary for the biogenesis of the endolysosomal system in vivo. *Nature*. 2012;485(7399):465-470.
18. Bucci C, Thomsen P, Nicoziani P, McCarthy J, van Deurs B. Rab7: a key to lysosome biogenesis. *Mol Biol Cell*. 2000;11(2):467-480.
19. Rink J, Ghigo E, Kalaidzidis Y, Zerial M. Rab conversion as a mechanism of progression from early to late endosomes. *Cell*. 2005;122(5):735-749.
20. Huotari J, Helenius A. Endosome maturation. *EMBO J*. 2011;30(17):3481-3500.

Downloaded from http://ashpublications.org/blood/article-pdf/doi/10.1182/blood.2020006871/1795769/blood.2020006871.pdf by HELMHOLTZ ZENTRUM user on 16 February 2021

21. Sönnichsen B, Renzis S de, Nielsen E, Rietdorf J, Zerial M. Distinct membrane domains on endosomes in the recycling pathway visualized by multicolor imaging of Rab4, Rab5, and Rab11. *J Cell Biol*. 2000;149(4):901-914.
22. van der Sluijs P, Hull M, Webster P, Mâle P, Goud B, Mellman I. The small GTP-binding protein rab4 controls an early sorting event on the endocytic pathway. *Cell*. 1992;70(5):729-740.
23. Ullrich O, Reinsch S, Urbé S, Zerial M, Parton RG. Rab11 regulates recycling through the pericentriolar recycling endosome. *J Cell Biol*. 1996;135(4):913-924.
24. Renzis S de, Sönnichsen B, Zerial M. Divalent Rab effectors regulate the sub-compartmental organization and sorting of early endosomes. *Nat Cell Biol*. 2002;4(2):124-133.
25. Nielsen E, Christoforidis S, Uttenweiler-Joseph S, Miaczynska M, Dewitte F, Wilm M, Hoflack B, Zerial M. Rabenosyn-5, a novel Rab5 effector, is complexed with hVPS45 and recruited to endosomes through a FYVE finger domain. *J Cell Biol*. 2000;151(3):601-612.
26. Jahn R, Lang T, Südhof TC. Membrane Fusion. *Cell*. 2003;112(4):519-533.
27. Dulubova I, Yamaguchi T, Gao Y, Min S-W, Huryeva I, Südhof TC, Rizo J. How Tlg2p/syntaxin 16 'snares' Vps45. *EMBO J*. 2002;21(14):3620-3631.
28. Tall GG, Hama H, DeWald DB, Horazdovsky BF. The phosphatidylinositol 3-phosphate binding protein Vac1p interacts with a Rab GTPase and a Sec1p homologue to facilitate vesicle-mediated vacuolar protein sorting. *Mol Biol Cell*. 1999;10(6):1873-1889.
29. Gengyo-Ando K, Kuroyanagi H, Kobayashi T, Murate M, Fujimoto K, Okabe S, Mitani S. The SM protein VPS-45 is required for RAB-5-dependent endocytic transport in Caenorhabditis elegans. *EMBO Rep*. 2007;8(2):152-157.
30. Morrison HA, Dionne H, Rusten TE, Brech A, Fisher WW, Pfeiffer BD, Celniker SE, Stenmark H, Bilder D. Regulation of Early Endosomal Entry by the Drosophila Tumor Suppressors Rabenosyn and Vps45. *Mol Biol Cell*. 2008;19(10):4167-4176.
31. Nichols BJ, Holthuis JC, Pelham HR. The Sec1p homologue Vps45p binds to the syntaxin Tlg2p. *Eur J Cell Biol*. 1998;77(4):263-268.
32. Bryant NJ, Piper RC, Gerrard SR, Stevens TH. Traffic into the prevacuolar/endosomal compartment of Saccharomyces cerevisiae: A VPS45-dependent intracellular route and a VPS45-independent, endocytic route. *Eur J Cell Biol*. 1998;76(1):43-52.
33. Cowles CR, Emr SD, Horazdovsky BF. Mutations in the VPS45 gene, a SEC1 homologue, result in vacuolar protein sorting defects and accumulation of membrane vesicles. *J Cell Sci*. 1994;107 (Pt 12):3449-3459.
34. Piper RC, Whitters EA, Stevens TH. Yeast Vps45p is a Sec1p-like protein required for the consumption of vacuole-targeted, post-Golgi transport vesicles. *Eur J Cell Biol*. 1994;65(2):305-318.
35. Rahajeng J, Caplan S, Naslavsky N. Common and distinct roles for the binding partners Rabenosyn-5 and Vps45 in the regulation of endocytic trafficking in mammalian cells. *Exp Cell Res*. 2009;316(5):859-874.
36. Pryor PR, Mullock BM, Bright NA, Gray SR, Luzio JP. The role of intraorganellar Ca(2+) in late endosome-lysosome heterotypic fusion and in the reformation of lysosomes from hybrid organelles. *J Cell Biol*. 2000;149(5):1053-1062.
37. Poole B, Ohkuma S. Effect of weak bases on the intralysosomal pH in mouse peritoneal macrophages. *J Cell Biol*. 1981;90(3):665-669.
38. Pless DD, Wellner RB. In vitro fusion of endocytic vesicles: effects of reagents that alter endosomal pH. *J Cell Biochem*. 1996;62(1):27-39.
39. Irandoust MI, Aarts LHJ, Roovers O, Gits J, Erkeland SJ, Touw IP. Suppressor of cytokine signaling 3 controls lysosomal routing of G-CSF receptor. *EMBO J*. 2007;26(7):1782-1793.

Downloaded from http://ashpublications.org/blood/article-pdf/doi/10.1182/blood.2020006871/1795769/blood.2020006871.pdf by HELMHOLTZ ZENTRUM user on 16 February 2021

40. Tam PPL, Loebel DAF. Gene function in mouse embryogenesis: get set for gastrulation. *Nat Rev Genet*. 2007;8(5):368-381.
41. Caza M, Hu G, Nielson ED, Cho M, Jung WH, Kronstad JW. The Sec1/Munc18 (SM) protein Vps45 is involved in iron uptake, mitochondrial function and virulence in the pathogenic fungus Cryptococcus neoformans. *PLoS Pathog*. 2018;14(8):e1007220.
42. Navaroli DM, Bellvé KD, Standley C, Lifshitz LM, Cardia J, Lambright D, Leonard D, Fogarty KE, Corvera S. Rabenosyn-5 defines the fate of the transferrin receptor following clathrin-mediated endocytosis. *PNAS*. 2012;109(8):E471-80.
43. Naslavsky N, Boehm M, Backlund PS, Caplan S. Rabenosyn-5 and EHD1 interact and sequentially regulate protein recycling to the plasma membrane. *Mol Biol Cell*. 2004;15(5):2410-2422.
44. Lin SX, Grant B, Hirsh D, Maxfield FR. Rme-1 regulates the distribution and function of the endocytic recycling compartment in mammalian cells. *Nat Cell Biol*. 2001;3(6):567-572.
45. Tang BL, Low DY, Lee SS, Tan AE, Hong W. Molecular cloning and localization of human syntaxin 16, a member of the syntaxin family of SNARE proteins. *Biochem Biophys Res Commun*. 1998;242(3):673-679.
46. Saint-Pol A, Yélamos B, Amessou M, Mills IG, Dugast M, Tenza D, Schu P, Antony C, McMahon HT, Lamaze C, Johannes L. Clathrin Adaptor epsinR Is Required for Retrograde Sorting on Early Endosomal Membranes. *Dev Cell*. 2004;6(4):525-538.
47. Shah RK, Munson M, Wierenga KJ, Pokala HR, Newburger PE, Crawford D. A novel homozygous VPS45 p.P468L mutation leading to severe congenital neutropenia with myelofibrosis. *Pediatr Blood Cancer*. 2017;64(9).
48. Magoulas PL, Shchelochkov OA, Bainbridge MN, Ben-Shachar S, Yatsenko S, Potocki L, Lewis RA, Searby C, Marcogliese AN, Elghetany MT, Zapata G, Hernández PP, Gadkari M, Einhaus D, Muzny DM, Gibbs RA, Bertuch AA, Scott DA, Corvera S, Franco LM. Syndromic congenital myelofibrosis associated with a loss-of-function variant in RBSN. *Blood*. 2018;132(6):658-662.
49. Stockler S, Corvera S, Lambright D, Fogarty K, Nosova E, Leonard D, Steinfeld R, Ackerley C, Shyr C, Au N, Selby K, van Allen M, Vallance H, Wevers R, Watkins D, Rosenblatt D, Ross CJ, Conibear E, Wasserman W, van Karnebeek C. Single point mutation in Rabenosyn-5 in a female with intractable seizures and evidence of defective endocytotic trafficking. *Orphanet J Rare Dis*. 2014;9:141.
50. Kolehmainen J, Black GCM, Saarinen A, Chandler K, Clayton-Smith J, Träskelin A-L, Perveen R, Kivitie-Kallio S, Norio R, Warburg M, Fryns J-P, La Chapelle Ad, Lehesjoki A-E. Cohen Syndrome Is Caused by Mutations in a Novel Gene, COH1, Encoding a Transmembrane Protein with a Presumed Role in Vesicle-Mediated Sorting and Intracellular Protein Transport. *Am J Hum Genet*. 2003;72(6):1359-1369.
51. Ménasché G, Pastural E, Feldmann J, Certain S, Ersoy F, Dupuis S, Wulffraat N, Bianchi D, Fischer A, Le Deist F, Saint Basile G de. Mutations in RAB27A cause Griscelli syndrome associated with haemophagocytic syndrome. *Nat Genet*. 2000;25(2):173-176.
52. Bohn G, Allroth A, Brandes G, Thiel J, Glocker E, Schäffer AA, Rathinam C, Taub N, Teis D, Zeidler C, Dewey RA, Geffers R, Buer J, Huber LA, Welte K, Grimbacher B, Klein C. A novel human primary immunodeficiency syndrome caused by deficiency of the endosomal adaptor protein p14. *Nat Med*. 2007;13(1):38-45.

Downloaded from http://ashpublications.org/blood/article-pdf/doi/10.1182/blood.2020006871/1795769/blood.2020006871.pdf by HELMHOLTZ ZENTRUM user on 16 February 2021

Figure Legends

Figure 1. VPS45 controls the intracellular organization of endolysosomal vesicles. (A) Immunoblot analysis of expression levels of VPS45 binding partners Rabenosyn-5 and Syntaxin16 in control and *VPS45* KO HeLa clones (n=3 different clones per genotype). One representative experiment of two independent experiments is shown. (B) Immunofluorescence microscopy analysis of control and *VPS45* KO HeLa clones to visualize early endosomes (EEA1), late endosomes (LAMP2), lysosomes (LAMP1) and the nucleus (DAPI). One representative experiment of three independent experiments is shown. Scale bars, 10 µm. (C) Immunoblot analysis of expression levels of EEA1, LAMP2 and LAMP1 in control and *VPS45* KO HeLa clones (n=3 different clones per genotype). One representative experiment of two independent experiments is shown.

Figure 2. VPS45 is dispensable for internalization but is required for efficient transferrin recycling. (A) Flow cytometric analysis of cargo uptake. Control and *VPS45* KO HeLa clones were incubated with 32.5 µg/ml fluorescent OVA at 37°C for indicated periods and the rate of cargo uptake was analyzed as a change in MFI from baseline (fluorescence at 4°C). Data are pooled from two independent experiments. Error bars indicate mean ± SD. Statistical analysis of significance using two-way ANOVA followed by Tukey´s multiple comparisons test revealed no significant difference in OVA uptake between control and *VPS45* KO HeLa clones. (B) Flow cytometric analysis of transferrin recycling in control and *VPS45* KO HeLa clones. Cells were incubated with 25 µg/ml of fluorescent transferrin for 30 minutes at 37°C, followed by a chase for the indicated periods and removal of surface-bound transferrin. Representative histograms of one control clone and one *VPS45* KO clone are shown. The chart shows cell-associated transferrin as the percentage of initial transferrin present at time t=0 and pooled data from four independent experiments are shown. Error bars indicate mean ± SD. Statistical analysis was performed using two-way ANOVA followed by Tukey´s multiple comparisons test. ns: not significant; ****, $p<0.0001$.

Downloaded from http://ashpublications.org/blood/article-pdf/doi/10.1182/blood.2020006871/1795769/blood.2020006871.pdf by HELMHOLTZ ZENTRUM user on 16 February 2021

Figure 3. *VPS45* KO cells fail to efficiently process soluble cargos and show a delayed maturation of cathepsin D. Control and *VPS45* KO HeLa clones were incubated with various fluorescent substrates for indicated time periods (A-B: DQ OVA, C: DQ Green BSA, D: pHrodo Green Dextran). (A) Representative confocal microscopy images of DQ OVA processing in control and *VPS45* KO HeLa clones are shown. After incubation with DQ OVA for 90 minutes, cells were fixed and stained for EEA1 and LAMP2. DAPI was used to visualize the nucleus. Zoom images represent magnified views of boxed areas (8 µm x 8 µm). One representative experiment of two independent experiments is shown. Scale bars, 10 µm. (B-D) The rate of substrate processing was determined by flow cytometry as a change in MFI from baseline (fluorescence at 4°C). (B) Control and *VPS45* KO cells were additionally treated with 25 µM chloroquine (CQ). Data are pooled from four independent experiments. (C) Data are pooled from three independent experiments. (D) Data are pooled from four independent experiments. (B-D) Error bars indicate mean ± SD. Statistical analysis was performed using two-way ANOVA followed by Tukey´s or Sidak's multiple comparisons test. ns: not significant; *, p<0.05; ***, p<0,001; ****, p<0.0001. (E) Expression levels of immature (50 kDa), intermediate (46 kDa), and mature (28 kDa) cathepsin D were analyzed in control and *VPS45* KO HeLa clones (n=3 different clones per genotype) by immunoblotting. One representative experiment of three independent experiments is shown.

Figure 4. Loss of VPS45 causes accumulation of EGFR in early endosomes and inefficient degradation. (A) Serum-starved control and *VPS45* KO HeLa clones were stimulated with 100 ng/ml EGF for indicated time periods and EGFR levels were analyzed by immunoblotting. One representative experiment of three independent experiments is shown. (B) Cells were treated as in (A), fixed and co-stained with anti-EGFR and anti-EEA1 antibodies. Nuclei were visualized using DAPI. Zoom images represent magnified views of boxed areas (10 µm x 10 µm) and profile blots along the dashed arrow (7 µm) are shown. One representative experiment of three independent experiments is shown. Scale bars, 10 µm. (C) Quantification of EGFR-EEA1 colocalization of data shown in (B). Pearson's correlation coefficient is plotted on the y-axis. For each genotype at least 40 cells were

Downloaded from http://ashpublications.org/blood/article-pdf/doi/10.1182/blood.2020006871/1795769/blood.2020006871.pdf by HELMHOLTZ ZENTRUM user on 16 February 2021

analyzed. Horizontal lines indicate the means and each symbol represents an individual cell. Statistical analysis was performed using two-way ANOVA with Tukey's multiple comparisons test. ****, p<0.0001.

Figure 5. VPS45 depletion results in prolonged association of G-CSFR with early endosomes and disrupted transport to late endosomes. (A) Serum-starved control and *VPS45* KO HeLa clones stably expressing G-CSFR-GFP fusion proteins were stimulated with 100 ng/ml G-CSF for 10 minutes, followed by a chase for the indicated periods. Stimulated cells were fixed and stained with anti-EEA1 and anti-LAMP2 antibodies. DAPI was used as a nuclear stain. Zoom images represent magnified views of boxed areas (10 µm x 10 µm). One representative experiment of two independent experiments is shown. Scale bars, 10 µm. (B) Quantification of G-CSFR-EEA1 and G-CSFR-LAMP2 co-localization of data shown in (A). Pearson's correlation coefficient is plotted on the y-axis. For each genotype at least 100 cells were analyzed. Horizontal lines indicate the means and each symbol represents an individual cell. Statistical analysis was performed using two-way ANOVA with Tukey's multiple comparisons test. ns: not significant; ****, p<0.0001.

Figure 6. Loss of VPS45 leads to a defective early-to-late endosome maturation. Non-modified control and *VPS45* KO HeLa clones were transduced with recombinant lentiviral vectors to co-express mCherry-Rab5 and mCerulean-Rab7. Dynamic changes of Rab5-positive and Rab7-positive vesicles were imaged during the uptake and transport of fluorescent cargo (microspheres-633). (A) Representative images of cargo trafficking in single vesicles of control and *VPS45* KO clones are shown. Scale bars, 1 µm. (B) The corresponding total fluorescence traces of Rab5 (red) and Rab7 (green) over time averaged from five independent experiments are shown. For visualization purposes, only every second frame is shown for the first twelve minutes in *VPS45* KO clones. Error bars indicate mean ± SEM.

Figure 7. VPS45 is essential for mouse embryogenesis at an early stage. (A) Representative PCR-based genotyping results of postnatal progeny derived from *Vps45*

Downloaded from http://ashpublications.org/blood/article-pdf/doi/10.1182/blood.2020006871/1795769/blood.2020006871.pdf by HELMHOLTZ ZENTRUM user on 16 February 2021

heterozygous intercrosses. Primer sets 1 and 2 used to identify control and heterozygous (Het) mice are shown in Figure S5A. M: DNA marker. (B) Genotyping results of 148 postnatal pups derived from *Vps45* heterozygous intercrosses. (C) A representative uterus derived from heterozygous intercrosses dissected at E13. Arrowheads show smaller implantation sites, indicating embryos that either died or were severely delayed in development. Scale bar, 5 mm. (D) Representative pictures of excised embryos derived from *Vps45* heterozygous intercrosses at E13, E11, and E7.5. Scale bars, 5 mm. (E) PAS-stained cross-sections of paraffin-embedded E7.5 embryos derived from *Vps45* heterozygous intercrosses showing the embryonic ectoderm (EE), endoderm (EN), and mesoderm (ME). Scale bars, 1 mm.

Downloaded from http://ashpublications.org/blood/article-pdf/doi/10.1182/blood.2020006871/1795769/blood.2020006871.pdf by HELMHOLTZ ZENTRUM user on 16 February 2021

Figure 1

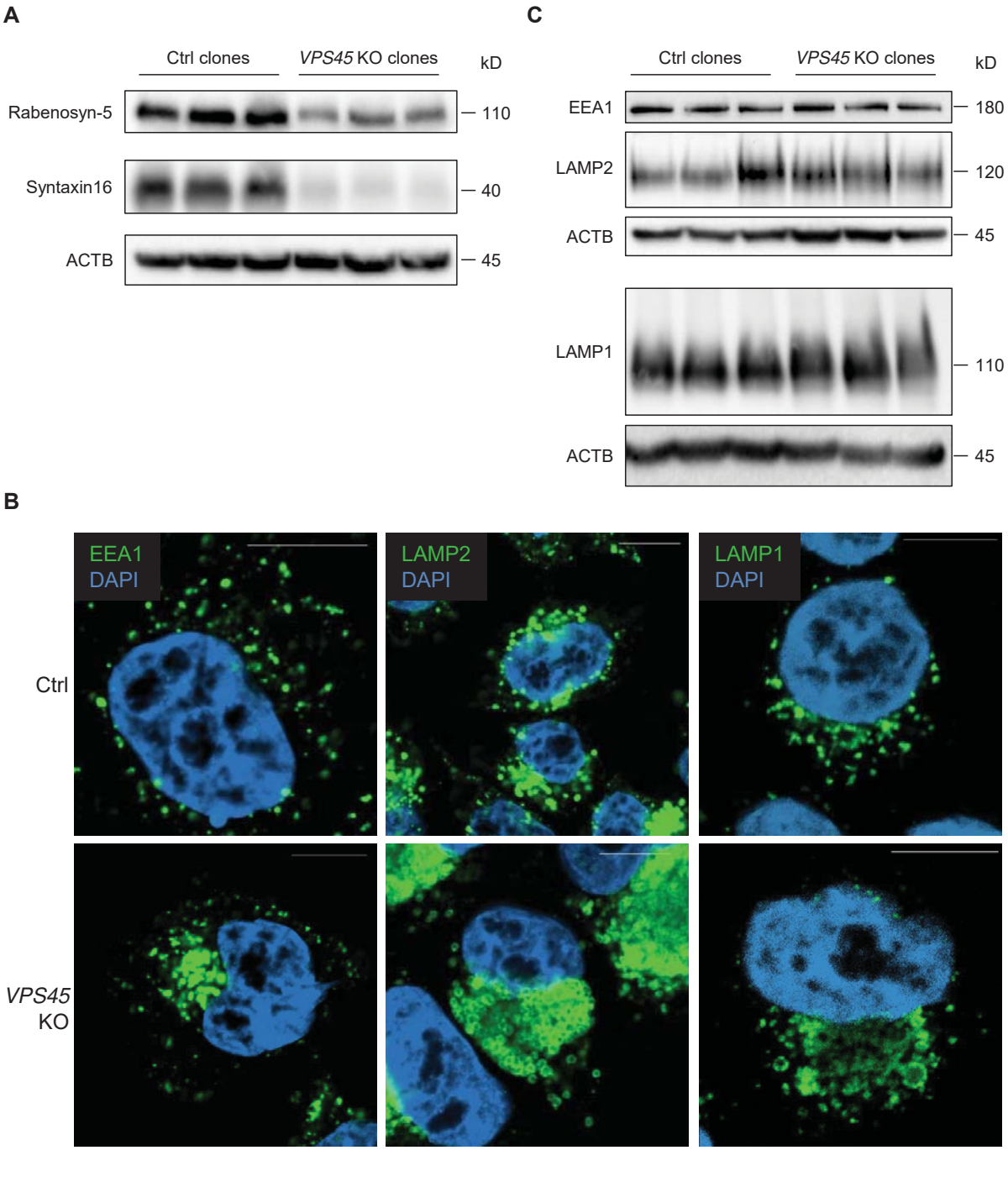

Downloaded from http://ashpublications.org/blood/article-pdf/doi/10.1182/blood.2020006871/1795769/blood.2020006871.pdf by HELMHOLTZ ZENTRUM user on 16 February 2021

Figure 2

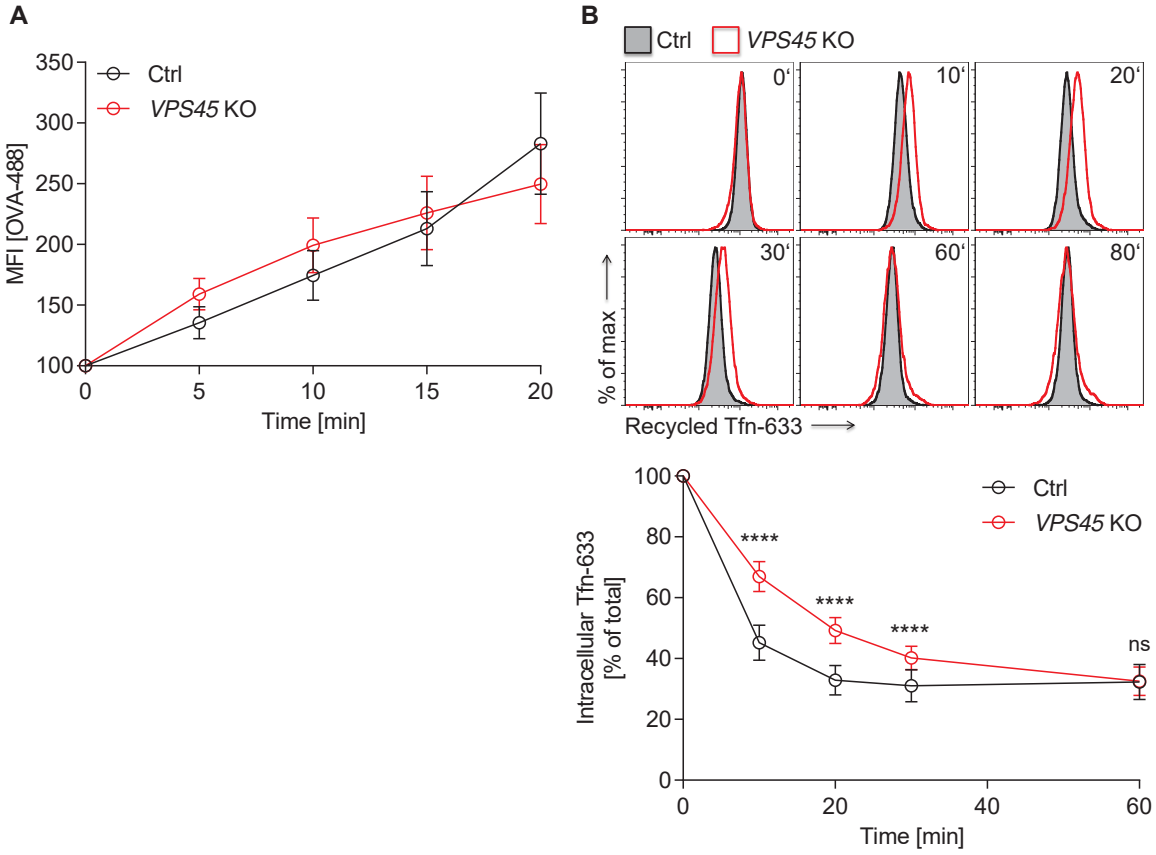

Downloaded from http://ashpublications.org/blood/article-pdf/doi/10.1182/blood.2020006871/1795769/blood.2020006871.pdf by HELMHOLTZ ZENTRUM user on 16 February 2021

Figure 3

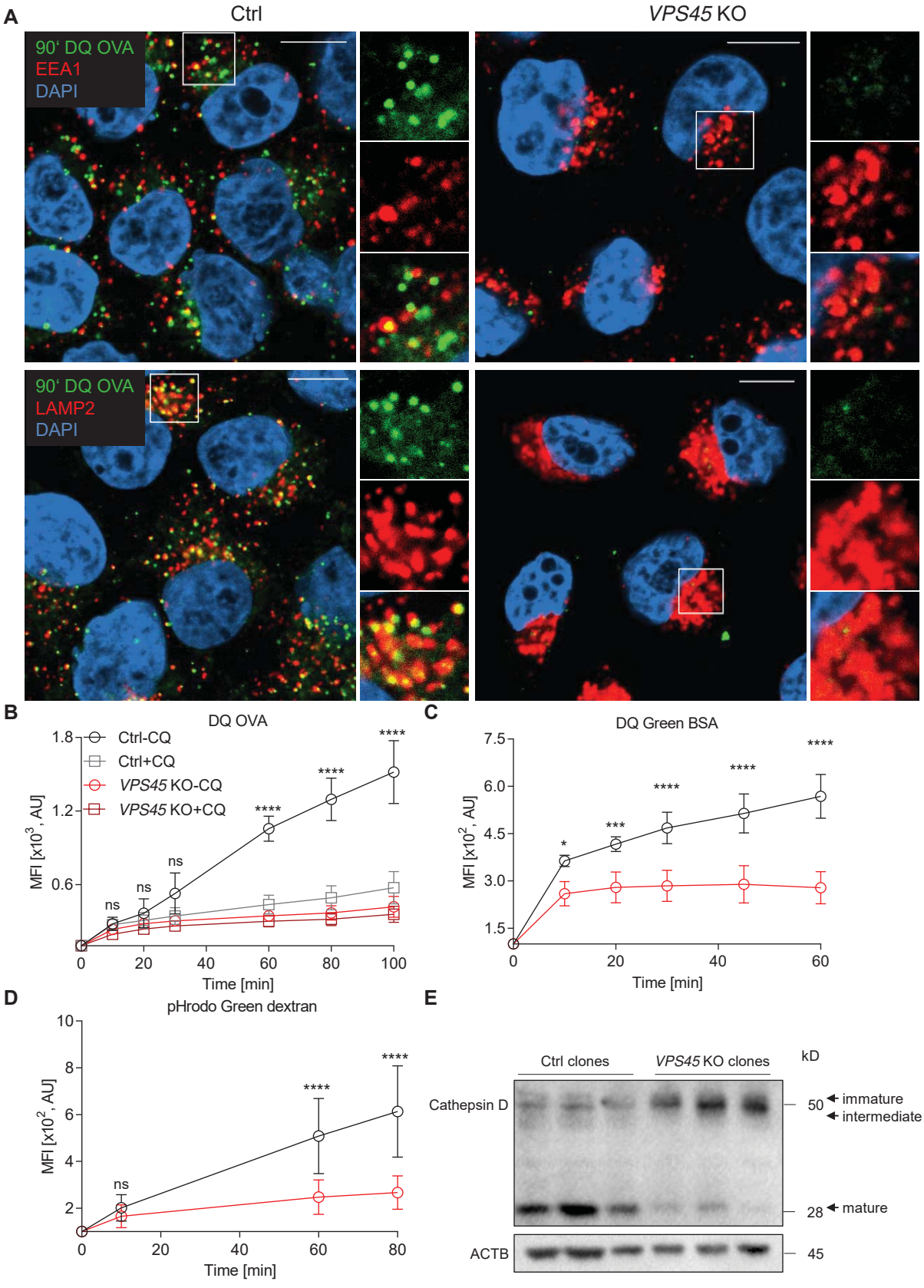

Downloaded from http://ashpublications.org/blood/article-pdf/doi/10.1182/blood.2020006871/1795769/blood.2020006871.pdf by HELMHOLTZ ZENTRUM user on 16 February 2021

Figure 4

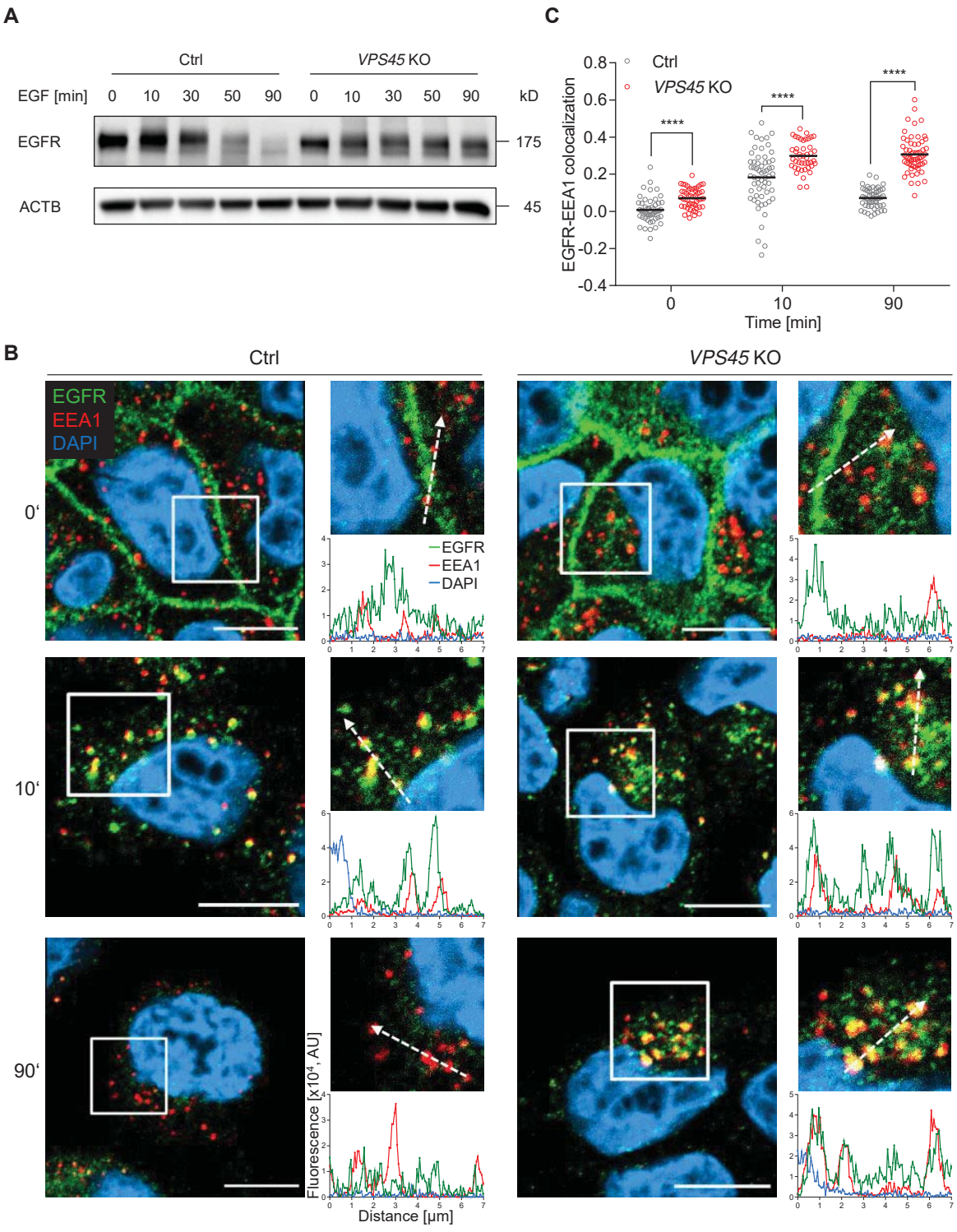

Downloaded from http://ashpublications.org/blood/article-pdf/doi/10.1182/blood.2020006871/1795769/blood.2020006871.pdf by HELMHOLTZ ZENTRUM user on 16 February 2021

Figure 5

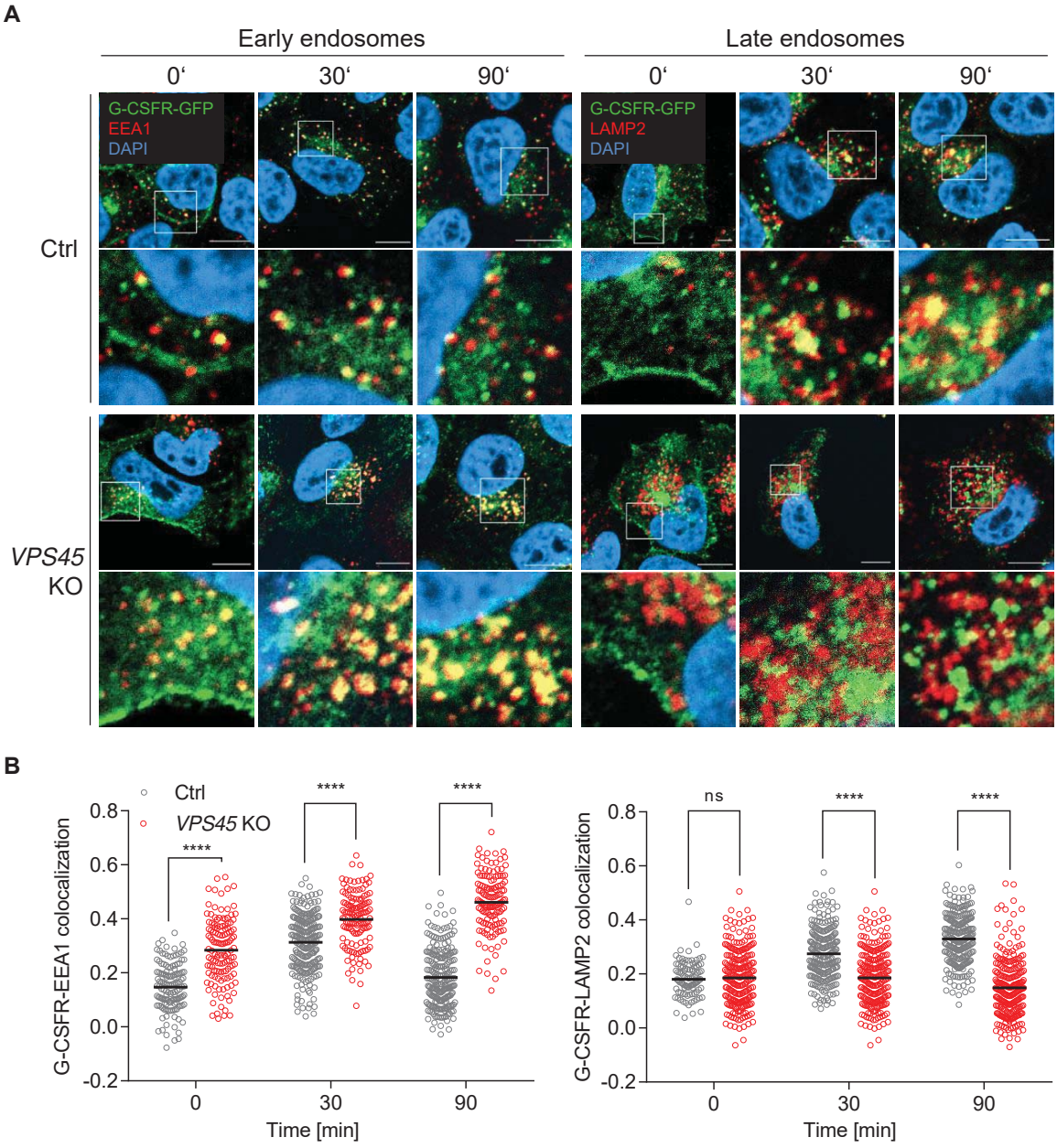

Downloaded from http://ashpublications.org/blood/article-pdf/doi/10.1182/blood.2020006871/1795769/blood.2020006871.pdf by HELMHOLTZ ZENTRUM user on 16 February 2021

Figure 6

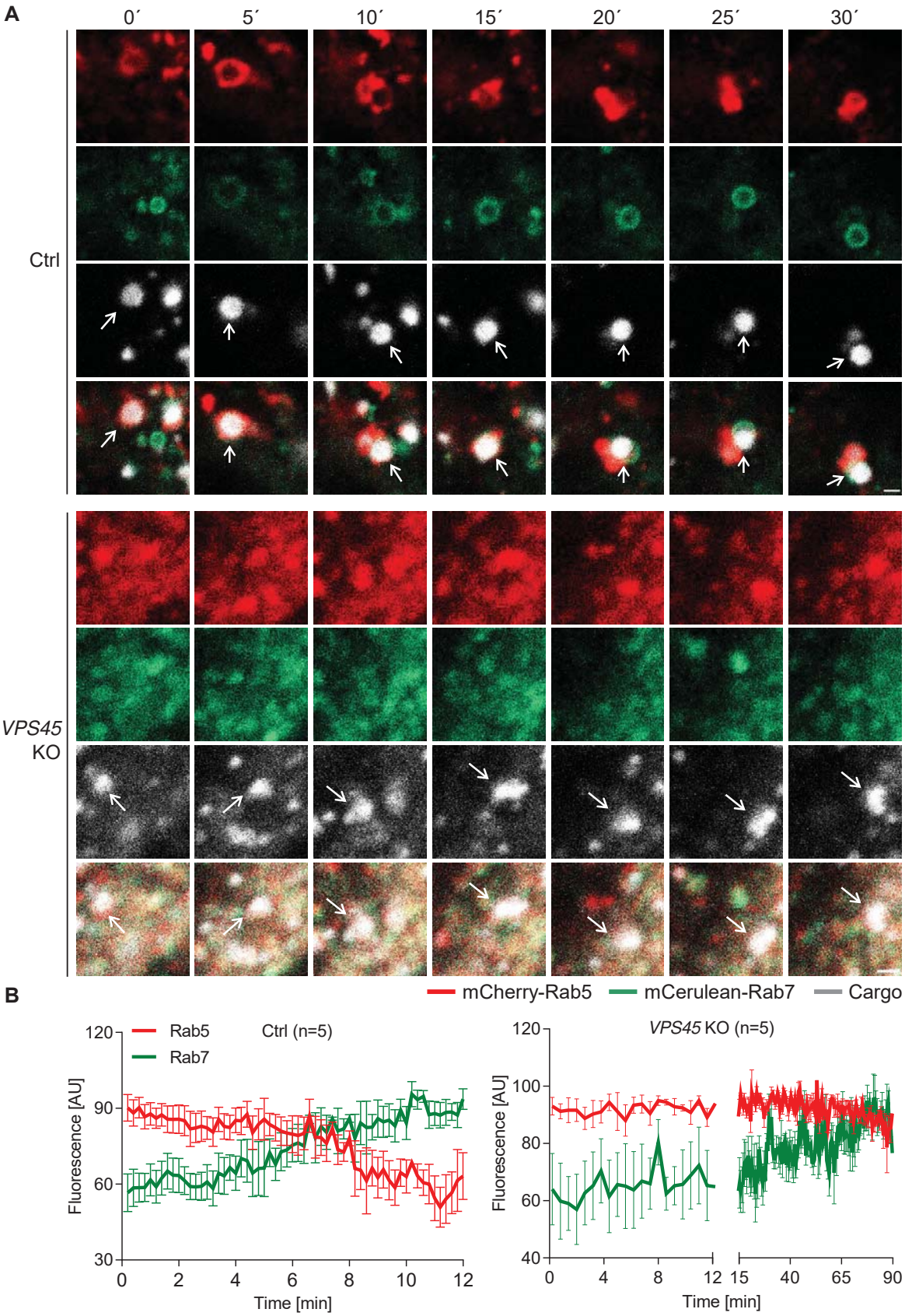

Downloaded from http://ashpublications.org/blood/article-pdf/doi/10.1182/blood.2020006871/1795769/blood.2020006871.pdf by HELMHOLTZ ZENTRUM user on 16 February 2021

Figure 7

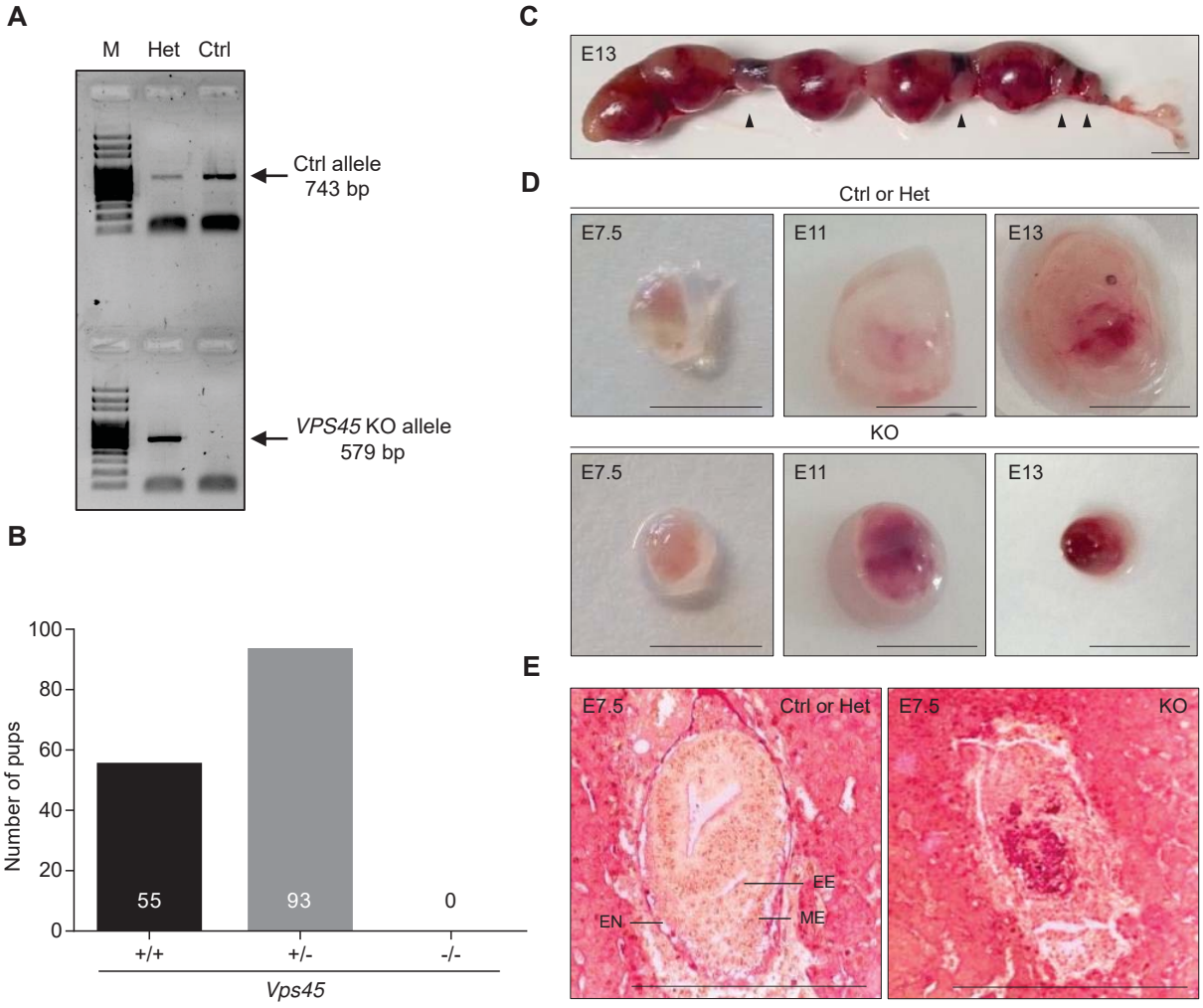

Downloaded from http://ashpublications.org/blood/article-pdf/doi/10.1182/blood.2020006871/1795769/blood.2020006871.pdf by HELMHOLTZ ZENTRUM user on 16 February 2021